J|A|C|S
ARTICLES
Published on Web 12/21/2002

Molecular Recognition in (+)-α-Pinene Oxidation by Cytochrome $P450_{cam}$

Stephen G. Bell,[†] Xuehui Chen,[‡] Rebecca J. Sowden,[†] Feng Xu,[‡] Jennifer N. Williams,[†] Luet-Lok Wong,*[,†] and Zihe Rao*[,‡]

Contribution from the Department of Chemistry, Inorganic Chemistry Laboratory, University of Oxford, South Parks Road, Oxford, OX1 3QR, U.K., and Laboratory of Structural Biology, School of Life Sciences and Engineering, Tsinghua University, Beijing 100084, China

Received September 8, 2002; E-mail: raoz@xtal.tsinghua.edu.cn; luet.wong@chem.ox.ac.uk

Abstract: Oxygenated derivatives of the monoterpene (+)-α-pinene are found in plant essential oils and used as fragrances and flavorings. (+)-α-Pinene is structurally related to (+)-camphor, the natural substrate of the heme monooxygenase cytochrome $P450_{cam}$ from *Pseudomonas putida*. The aim of the present work was to apply the current understanding of P450 substrate binding and catalysis to engineer $P450_{cam}$ for the selective oxidation of (+)-α-pinene. Consideration of the structures of (+)-camphor and (+)-α-pinene lead to active-site mutants containing combinations of the Y96F, F87A, F87L, F87W, and V247L mutations. All mutants showed greatly enhanced binding and rate of oxidation of (+)-α-pinene. Some mutants had tighter (+)-α-pinene binding than camphor binding by the wild-type. The most active was the Y96F/V247L mutant, with a (+)-α-pinene oxidation rate of 270 nmol (nmol of $P450_{cam}$)$^{-1}$ min^{-1}, which was 70% of the rate of camphor oxidation by wild-type $P450_{cam}$. Camphor is oxidized by wild-type $P450_{cam}$ exclusively to 5-*exo*-hydroxycamphor. If the gem dimethyl groups of (+)-α-pinene occupied similar positions to those found for camphor in the wild-type structure, (+)-*cis*-verbenol would be the dominant product. All $P450_{cam}$ enzymes studied gave (+)-*cis*-verbenol as the major product but with much reduced selectivity compared to camphor oxidation by the wild-type. (+)-Verbenone, (+)-myrtenol, and the (+)-α-pinene epoxides were among the minor products. The crystal structure of the Y96F/F87W/V247L mutant, the most selective of the $P450_{cam}$ mutants initially examined, was determined to provide further insight into $P450_{cam}$ substrate binding and catalysis. (+)-α-Pinene was bound in two orientations which were related by rotation of the molecule. One orientation was similar to that of camphor in the wild-type enzyme while the other was significantly different. Analysis of the enzyme/substrate contacts suggested rationalizations of the product distribution. In particular competition rather than cooperativity between the F87W and V247L mutations and substrate movement during catalysis were proposed to be major factors. The crystal structure lead to the introduction of the L244A mutation to increase the selectivity of pinene oxidation by further biasing the binding orientation toward that of camphor in the wild-type structure. The F87W/Y96F/L244A mutant gave 86% (+)-*cis*-verbenol and 5% (+)-verbenone. The Y96F/L244A/V247L mutant gave 55% (+)-*cis*-verbenol but interestingly also 32% (+)-verbenone, suggesting that it may be possible to engineer a $P450_{cam}$ mutant that could oxidize (+)-α-pinene directly to (+)-verbenone. Verbenol, verbenone, and myrtenol are naturally occurring plant fragrance and flavorings. The preparation of these compounds by selective enzymatic oxidation of (+)-α-pinene, which is readily available in large quantities, could have applications in synthesis. The results also show that the protein engineering of $P450_{cam}$ for high selectivity of substrate oxidation is more difficult than achieving high substrate turnover rates because of the subtle and dynamic nature of enzyme−substrate interactions.

Introduction

Terpenes have the general formula $(C_5H_8)_n$ and are biosynthesized from isoprene units in the form of isopentenyl pyrophosphate.[1] After the head-to-head and head-to-tail coupling of isoprene units, a series of carbonium ion rearrangements leads to a wide variety of cyclic and acyclic terpene skeletal structures.The parent terpenes and their oxidation products, such as the epoxides, alcohols, aldehydes, and ketones, constitute one of largest class of organic compounds found in biological systems. Monoterpenes ($n = 2$) are more volatile than their sesquiterpenoid ($n = 3$) homologues. The involatile diterpenes such as squalene ($n = 4$) and larger terpenoids have important biological activities; e.g., some are hormones or precursors to hormones.

Many mono- and sesquiterpenoid compounds found naturally in plant essential oils are sought-after fragrances and flavorings due to their distinctive, pleasant odors and taste notes.[2,3] For example (−)-menthol, which gives peppermint the characteristic cooling sensation, (−)-carvone, which gives the spearmint

[†] University of Oxford.
[‡] Tsinghua University.

(1) Gershenzon, J.; Croteau, R. B. *Lipid Metab. Plants* **1993**, 339−388.

flavor, and (−)-perillyl aldehyde, found in the herb *perilla*, are derived from the monoterpene (−)-limonene. The highly specific cytochrome P450 monooxygenases (CYP71D18 from spearmint and CYP71D13 from peppermint), which catalyze the initial oxidation of (−)-limonene in the respective plants, have been expressed and their properties investigated extensively.[4−9] Verbenol, verbenone, and myrtenol are derived from the oxidation of α-pinene. However, the enzymes involved in biological α-pinene oxidation are not yet well characterized.[10−12] The desirable properties of monooxygenated terpenoids meant that they are high added-value fine chemicals. The one-step or one-pot synthesis of these compounds by direct oxidation of the readily available parent terpenes could therefore have applications in synthesis.

Cytochrome $P450_{cam}$ (CYP101)[13,14] from the soil bacterium *Pseudomonas putida* catalyzes the oxidation of (+)-camphor to 5-*exo*-hydroxycamphor, the first step in the camphor metabolism pathway of the organism.[15,16] The $P450_{cam}$ system has been studied extensively,[17] and the crystal structure of different forms of the enzyme with a variety of molecules bound within the active site have been determined.[18−29] The bicyclic compound (+)-α-pinene is structurally related to camphor (Figure 1). We are interested in the possibility of applying the current knowledge of $P450_{cam}$ substrate binding and recognition, mechanism, and dynamics to engineer the enzyme for the selective oxidation of (+)-α-pinene. Such engineered variants may have applications in synthesis and also could provide a means for discovering compounds with novel biological properties.

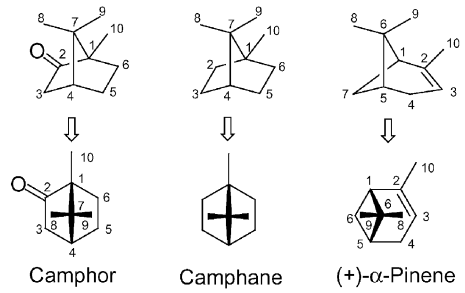

Figure 1. Molecular structures of (+)-camphor, (+)-camphane, and (+)-α-pinene.

In the present study, we designed a number of active-site mutations based on a comparison of the structures of camphor and (+)-α-pinene. The activity, selectivity, and coupling efficiency of these $P450_{cam}$ mutants for (+)-α-pinene oxidation were assayed. We also determined the crystal structure of the F87W/Y96F/V247L triple mutant with (+)-α-pinene bound within the active site. Based on the enzyme/substrate contacts revealed by the structure, and the results of the activity studies, further mutations were carried out and improved selectivity for the formation of (+)-*cis*-verbenol was obtained.

Materials and Methods

The atomic coordinates have been deposited in the Protein Data Bank, code 1MPW.

General Materials. Enzymes for molecular biology were from New England Biolabs. Buffer components were from Anachem Ltd. General reagents were from Sigma-Aldrich or Merck. NADH was from Roche Diagnostics. (+)-α-Pinene, α-pinene epoxide, (−)-*cis*-verbenol, (+)-myrtenol, (+)-perillyl alcohol, and (−)-carvone were from Sigma-Aldrich. UV/vis spectra were recorded on a CARY 1E double-beam spectrophotometer equipped with a Peltier cell temperature controller (±0.1 °C). Gas chromatographic (GC) analyses were performed on a Fisons 8000 series instrument equipped with a flame-ionization detector (FID). Two columns were used, a DB-1 fused silica capillary column (0.25 mm i.d. × 30 m) for general analysis and a β-DEX chiral phase column (0.5 mm i.d. × 30 m) for the separation of optical isomers.

Enzymes and Molecular Biology. General DNA and microbiological manipulations were carried out by standard methods.[30] Cytochrome $P450_{cam}$ and its associated electron-transfer proteins putidaredoxin and putidaredoxin reductase were expressed in *Escherichia coli* and purified following standard methods.[31−33] The purified proteins were stored at −20 °C in buffers containing 50% glycerol. Immediately before use the proteins were buffer exchanged into 50 mM Tris, pH 7.4, on a 5-mL bed volume PD-10 gel filtration column (Amersham Biosciences). Site-directed mutagenesis was carried out by using the Stratagene QuikChange mutagenesis kit with oligonucleotide primers designed following the manufacturer's guidelines. Some mutants were prepared by cloning fragments of the $P450_{cam}$ gene from different mutants using

(2) Arctander, S. *Perfume and Flavor Materials of Natural Origin*; Allured Publ. Co.: Wheaton, IL, 1960.
(3) Charlwood, B. V.; Charlwood, K. A. *Methods Plant Biochem.* **1991**, *7*, 43−98.
(4) Karp, F.; Mihaliak, C. A.; Harris, J. L.; Croteau, R. *Arch. Biochem. Biophys.* **1990**, *276*, 219−226.
(5) Haudenschild, C.; Schalk, M.; Karp, F.; Croteau, R. *Arch. Biochem. Biophys.* **2000**, *379*, 127−136.
(6) Wust, M.; Little, D. B.; Schalk, M.; Croteau, R. *Arch. Biochem. Biophys.* **2001**, *387*, 125−136.
(7) Wust, M.; Croteau, R. B. *Biochemistry* **2002**, *41*, 1820−1827.
(8) Schalk, M.; Croteau, R. *Proc. Natl. Acad. Sci. U. S. A.* **2000**, *97*, 11 948−11 953.
(9) Lupien, S.; Karp, F.; Wildung, M.; Croteau, R. *Arch. Biochem. Biophys.* **1999**, *368*, 181−192.
(10) Colocousi, A.; Leak, D. J. *Environ. Biotechnol.* **1996**, 144−157.
(11) Niku-Paavola, M. L.; Viikari, L. *J. Mol. Catal. B: Enzymol.* **2000**, *10*, 435−444.
(12) Savithiry, N.; Gage, D.; Fu, W.; Oriel, P. *Biodegradation* **1998**, *9*, 337−341.
(13) Nebert, D. W.; Nelson, D. R.; Coon, M. J.; Estabrook, R. W.; Feyereisen, R.; Fujii-Kuriyama, Y.; Gonzalez, F. J.; Guengerich, F. P.; Gunsalus, I. C.; Johnson, E. F.; Loper, J. C.; Sato, R.; Waterman, M. R.; Waxman, D. J. *DNA Cell Biol.* **1991**, *10*, 1−14.
(14) Nelson, D. R.; Koymans, L.; Kamataki, T.; Stegeman, J. J.; Feyereisen, R.; Waxman, D. J.; Waterman, M. R.; Gotoh, O.; Coon, M. J.; Estabrook, R. W.; Gunsalus, I. C.; Nerbert, D. W. *Pharmacogenetics* **1996**, *6*, 1−42.
(15) Gunsalus, I. C.; Wagner, G. C. *Methods Enzymol.* **1978**, *52*, 166−188.
(16) Sligar, S. G.; Murray, R. I. In *Cytochrome P450: Structure, Mechanism, and Biochemistry*, 1st ed.; Ortiz de Montellano, P. R., Ed.; Plenum Press: New York, 1986; pp 429−503.
(17) Mueller, E. J.; Loida, P. J.; Sligar, S. G. In *Cytochrome P450: Structure, Mechanism, and Biochemistry*, 2nd ed.; Ortiz de Montellano, P. R., Ed.; Plenum Press: New York, 1995; pp 83−124.
(18) Poulos, T. L.; Finzel, B. C.; Gunsalus, I. C.; Wagner, G. C.; Kraut, J. *J. Biol. Chem.* **1985**, *260*, 16 122−16 130.
(19) Poulos, T. L.; Finzel, B. C.; Howard, A. J. *Biochemistry* **1986**, *25*, 5314−5322.
(20) Poulos, T. L.; Finzel, B. C.; Howard, A. J. *J. Mol. Biol.* **1987**, *195*, 687−700.
(21) Raag, R.; Poulos, T. L. *Biochemistry* **1989**, *28*, 7586−7592.
(22) Raag, R.; Poulos, T. L. *Biochemistry* **1991**, *30*, 2674−2684.
(23) Raag, R.; Poulos, T. L. *Biochemistry* **1989**, *28*, 917−922.
(24) Vidakovic, M.; Sligar, S. G.; Li, H.; Poulos, T. L. *Biochemistry* **1998**, *37*, 9211−9219.
(25) Raag, R.; Martinis, S. A.; Sligar, S. G.; Poulos, T. L. *Biochemistry* **1991**, *30*, 11420−11429.
(26) Schlichting, I.; Jung, C.; Schulze, H. *FEBS Lett.* **1997**, *415*, 253−257.
(27) Schlichting, I.; Berendzen, J.; Chu, K.; Stock, A. M.; Maves, S. A.; Benson, D. E.; Sweet, R. M.; Ringe, D.; Petsko, G. A.; Sligar, S. G. *Science* **2000**, *287*, 1615−1622.
(28) Di Gleria, K.; Nickerson, D. P.; Hill, H. A. O.; Wong, L.-L.; Fülöp, V. *J. Am. Chem. Soc.* **1998**, *120*, 46−52.
(29) Li, H.; Narasimhulu, S.; Havran, L. M.; Winkler, J. D.; Poulos, T. L. *J. Am. Chem. Soc.* **1995**, *117*, 6297−6299.
(30) Sambrook, J.; Fritsch, E. F.; Maniatis, T. *Molecular Cloning: A Laboratory Manual*, 2nd ed.; Cold Spring Harbor Laboratory Press: New York, 1989.
(31) Westlake, A. C.; Harford-Cross, C. F.; Donovan, J.; Wong, L. L. *Eur. J. Biochem.* **1999**, *265*, 929−935.
(32) Peterson, J. A.; Lorence, M. C.; Amarneh, B. *J. Biol. Chem.* **1990**, *265*, 6066−6073.
(33) Yasukochi, T.; Okada, O.; Hara, T.; Sagara, Y.; Sekimizu, K.; Horiuchi, T. *Biochim. Biophys. Acta* **1994**, *1204*, 84−90.

the unique *Nde* I restriction site at the 5′-end of the gene, the internal *Sph* I site which spanned amino acids 121−123, and the *Hin*d III site at the 3′-end of the gene. Thus the Y96F/ L224A/V247L mutant was generated by ligating together the *Nde* I/*Sph* I fragment of the Y96F mutant (which contained the Y96F mutation) with the *Sph* I/*Hin*d III fragment of the F87W/Y96F/L224A/V247L mutant (containing the L244A and V247L mutations). Mutants were identified and fully sequenced by automated DNA sequencing on an ABI 377XL Prism DNA sequencer by the DNA sequencing facility at the Department of Biochemistry, University of Oxford. All $P450_{cam}$ enzymes described in this work also contained the C334A mutation to prevent protein dimerization via disulfide bond formation.[34] For convenience, the C334A base mutant is referred to as "wild-type", the triple mutant F87W/Y96F/C334A as F87W/Y96F, etc.

$P450_{cam}$ Crystallization and Substrate Soaking Experiments. Crystals of the F87W/Y96F/V247L mutant were grown at 291 K by the vapor diffusion method. Immediately prior to crystallization the mutant was further purified by size-exclusion chromatography on a Superdex 75 (Amersham Biosciences) column (26 mm i.d. × 80 cm) by eluting with 40 mM phosphate, pH 7.4, containing 1 mM camphor, 10 mM β-mercaptoethanol, and 200 mM KCl. The column was eluted at a flow rate of 0.8 mL min^{-1}, and orange-red $P450_{cam}$ fractions with $A_{404}/A_{280} \geq 1.1$ were pooled and used for crystallization. The protein was buffer exchanged into 100 mM cacodylate, pH 6.5, and 200 mM KCl and concentrated to 8 mg mL^{-1} by ultrafiltration. A 1-μL aliquot of this solution was mixed with 1 μL of 30% PEG8000 in buffer A (100 mM cacodylate, pH 6.5, 200 mM sodium acetate) and suspended over 1 mL of 18−24% PEG8000 in buffer A. Diffraction quality crystals of $P450_{cam}$ appeared within 24 h. Crystals were captured with a fiber loop and soaked in 100 mM MES, pH 6.5, 100 mM sodium acetate, 100 mM KCl, and 20% PEG8000 containing 100 μM (+)-α-pinene (added as a 100 mM stock in ethanol) for 5 days.

Data Collection and Structure Refinement. Immediately prior to data collection, crystals were soaked in a cryoprotecting solution consisting of 100 mM MES, pH 6.5, 100 mM KCl, 100 mM sodium acetate, 20% glycerol, and 20% PEG8000 and flash frozen at 100 K in a stream of cold nitrogen gas. X-ray diffraction data were collected at 100 K on a MAR345 image plate by using Cu Kα radiation ($\lambda = 1.5418$ Å) from an in-house Rigaku rotating anode X-ray generator operating at 48 kV and 98 mA. The crystals belonged to the space group $P2_1$ with unit cell dimensions $a = 66.90$ Å, $b = 62.52$ Å, $c = 95.70$ Å, and $\beta = 90.28°$. A total of 300 428 reflections were measured, with a R_{merge} of 8.6% for 33 002 unique reflections and 97.1% completeness (50−2.3 Å). Data were collected to 84.3% completeness in the highest resolution shell.

The structure was solved by molecular replacement based on the crystal structure of wild-type $P450_{cam}$ with bound camphor (protein databank code: 2CPP). In the case of the mutant crystal, although the three angles of the unit cell were all virtually 90°, R_{sym} in the orthorhombic system was considerably higher than for a monoclinic cell, especially in higher resolution shells. More importantly, extensive molecular replacement was attempted in all possible orthorhombic space groups without any success. Hence the mutant was determined to be of $P2_1$ space group for which we were able to find two molecular replacement solutions corresponding to the two molecules per asymmetric unit. The $P2_1$ space group was also found to be the case in a similar study.[27] The space group parameters suggested that the crystals have 222 pseudo-symmetry and this was further confirmed by inspection of the crystal packing. The two molecules in the same asymmetric unit were 62 Å apart with a rotation angle of 13.5° along an axis perpendicular to the *z* axis and at 97° to the *x* axis when superimposed. As evident in the difference Fourier map, both molecules showed clear electron density above the heme group, which could be modeled as (+)-α-pinene but with different substrate orientations. The final refinement parameters were $R_{work} = 19.4\%$ and $R_{free} = 26.0\%$. The data collection and structure refinement statistics are summarized in Table 1.

Table 1. X-ray Data Collection, Refinement, and Common Structural Parameters

	data
unit cell	$a = 66.90$ Å, $b = 62.52$ Å, $c = 95.70$ Å $\beta = 90.3°$
space group	$P21$
no. of molecules in unit cell	2 (**A**,**B**)
refinement	502.3 Å
total no. of reflections	300 428
unique reflections	33 002
completeness (highest resolution shell)	97.1% (84.3%)
$(I)/[\sigma(I)]$	20
R_{merge}[a]	8.6%
R_{work}[b]	19.4%
R_{free}[b]	26%
residues not modeled	A1−A9, B1−B9
no. of molecules with (+)-α-pinene bound	2 (**A**,**B**)
rmsd from restraint values	bond lengths 0.0016 Å bond angles 1.76°
rmsd between C_α backbone of molecules	WT vs **A** 0.39 Å; WT vs **B** 0.44 Å **A** vs **B** 0.36 Å
Fe−S (cysteine 357) distance	**A** 2.29 Å; **B** 2.08 Å; WT 2.20 Å
Fe−porphyrin plane distance	**A** 0.36 Å; **B** 0.36 Å; WT 0.37 Å
Ramachandran analysis: most favored (additionally allowed)	**A** 88.2% (11.8%); **B** 84.8% (15.2%)

[a] $R_{merge} = \Sigma|(I) - I|/\Sigma(I)$ over all reflections. [b] $R_{work} = \Sigma|F_o - F_c|/F_o$ for all reflections, R_{free} calculated from against 8% reflections withheld at random.

Substrate Binding Constant and NADH Turnover Rate Determinations. All (+)-α-pinene binding and oxidation assays were carried out at 30 °C. The substrate-free form of the $P450_{cam}$ enzymes, obtained by passage through a PD-10 gel filtration column, were diluted to 1 μM. KCl was added from a 2 M stock in 50 mM Tris, pH 7.4 buffer, to 200 mM. The substrate was added from ethanolic stocks and the spectra of the mixed high-spin/low-spin form of the enzyme at different pinene concentrations were recorded. Ethanol on its own at the final total concentration of ca. 5% did not induce any change in the spectra. The (+)-α-pinene binding constant was determined according to literature methods.[35]

Incubation mixtures for NADH turnover assays (1.5 mL) contained 50 mM Tris, pH 7.4, 200 mM KCl, 1 μM $P450_{cam}$, 4 μM putidaredoxin, 1 μM putidaredoxin reductase, and 30 $\mu g\ \mu L^{-1}$ bovine liver catalase.[36] The mixtures were oxygenated and then equilibrated at 30 °C for 2 min. The (+)-α-pinene substrate was added as a 100 mM stock in ethanol to a final concentration of 400 μM. NADH was added to 250 μM and the absorbance at 340 nm was monitored. The reaction mixtures were stirred throughout the time-course of the reaction. The maximum concentration of ethanol in an incubation reaction was 0.4% v/v, and control experiments showed that ethanol at concentrations up to 10% v/v did not induce any increase in NADH consumption above background.

Product Formation Rate Determinations. After all the NADH had been consumed in an incubation experiment, 1 mL of the mixture was transferred to a glass centrifuge tube. (−)-Carvone was added from a 10 mM stock in ethanol to 50 μM final concentration to act as an internal standard for the extraction and GC analysis steps. The organics were extracted by vortexing with 250 μL of prechilled (4 °C) chloroform. The phases were separated by centrifuging at 3500*g*,

(34) Nickerson, D. P.; Wong, L.-L. *Protein Eng.* **1997**, *10*, 1357−1361.

(35) Peterson, J. A. *Arch. Biochem. Biophys.* **1971**, *144*, 678−693.

(36) Stevenson, J.-A.; Westlake, A. C. G.; Whittock, C.; Wong, L.-L. *J. Am. Chem. Soc.* **1996**, *118*, 12846−12847.

4 °C, and the chloroform layer was carefully removed. The samples were either analyzed immediately or stored at −20 °C until required.

The organic extracts were analyzed by GC with the flame ionization detector set at 250 °C and the injector at 150 °C. The temperature of the DB-1 column was held at 120 °C. The retention times were as follows: pinene epoxides, 4.65 and 4.80 min; (+)-*cis*-verbenol, 5.25 min; (+)-myrtenol, 6.30 min; (+)-verbenone, 6.40 min. The DB-1 column did not have a chiral stationary phase and so would not separate the enantiomers of a chiral compound, e.g., (+)-*cis*-verbenol and (−)-*cis*-verbenol would have identical retention times, but diastereoisomers such as (+)-*cis*-verbenol and (+)-*trans*-verbenol were resolved. The chiral phase β-DEX column, on the other hand, resolved all isomers.

The concentration of (+)-α-pinene oxidation products in an incubation mixture was determined by calibration of the FID response for the products using (+)-perillyl alcohol as a representative example of oxygenated pinenes. The assumption was that these isomeric compounds would have near identical responses on the FID, and this was shown to be the case by comparing the GC peak areas of different solutions containing the same concentration of a number of mono-oxygenated terpenes including the alcohols, epoxides, and ketones. With this small caveat in mind, mixtures containing different concentrations of (+)-perillyl alcohol and all components of a reaction except NADH and the substrate were extracted and analyzed as described above. The ratio of the peak areas of (+)-perillyl alcohol and the internal standard was plotted against the (+)-perillyl alcohol concentration. This calibration plot was a straight line passing through the origin. The concentrations of the different products formed, and hence the total product formation rate, were readily determined from the plot. The coupling efficiency, defined as the proportion of NADH consumed that lead to product formation, was then readily calculated from the total product concentration and the amount of NADH added to initiate the reaction.

Characterization of Metabolites. The major (+)-α-pinene oxidation products were initially identified by GC coelution experiments with authentic samples. (+)-*cis*-Verbenol coeluted with (−)-*cis*-verbenol on the DB-1 column but not the β-DEX column, which partially identified the product. (+)-Myrtenol, (+)-verbenone, and the (+)-α-pinene epoxides were identified by coelution on both columns. To establish the identities of these compounds, a preparative scale oxidation reaction was carried out with the Y96F/ V247L mutant.[37] The products were separated by silica column chromatography, eluting with hexane/ethyl acetate mixtures. (+)-*cis*-Verbenol, (+)-verbenone, and (+)-myrtenol were all readily separated and purified. Their 500-MHz ^{1}H NMR spectra were in full agreement with those of authentic compounds. The diastereomers of the epoxide could not be separated but these had been positively identified by coelution with a racemic commercial sample. The other minor products could not be purified satisfactorily and were not characterized further.

Results and Discussion

Designing the Active Site Mutations. As shown in Figure 1, (+)-α-pinene is structurally related to camphor—camphor is a bicyclic-2,2,1 compound while (+)-α-pinene has the 3,1,1 structure. The carbonyl group in camphor is absent from (+)-α-pinene and the C_{10} methyl group is on a different ring carbon in (+)-α-pinene. We therefore set out to engineer the P450$_{cam}$ active site to compensate for these structural differences so as to promote (+)-α-pinene binding and oxidation.

In the crystal structure of wild-type P450$_{cam}$ with bound camphor (Figure 2), the C_8,C_9 methyl groups of the substrate are in van der Waals contact with the V295 side chain. Camphane was bound in a virtually identical orientation.[22] Our starting point for active-site engineering was the assumption

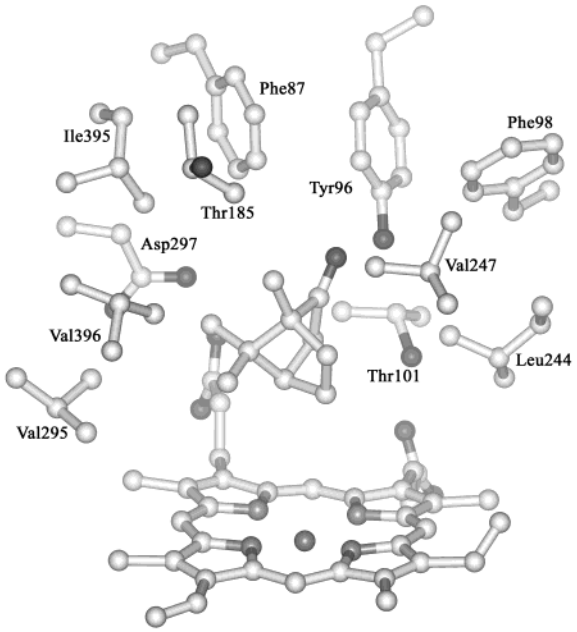

Figure 2. Active site structure of the monoclinic form of wild-type P450$_{cam}$ with camphor bound, crystallized from PEG8000.[27] The T101 side-chain orientation is the same as that observed in the present work but rotated by ca. 90° compared to the orthorhombic form.[20]

that (+)-α-pinene would also be bound with its C_8,C_9 methyl groups contacting V295, and the overall orientation would be approximately the same as that for camphor. The camphor carbonyl group forms a hydrogen bond with Y96 and it also contacts the F87 side chain.[20] Since this carbonyl group is absent from (+)-α-pinene, the Y96F mutation should improve pinene binding by removing the polar phenol side chain.[38] The larger side chain of the F87W mutation might improve the enzyme−substrate fit by "filling in" the space left as a result of the absence of the camphor carbonyl group in (+)-α-pinene. The effect of side-chain volume at the 87 position was also investigated with the F87A and F87L mutations. The C_{10} methyl group of camphor contacts the V247 side chain in the wild type.[20] Since the C_{10} methyl group of (+)-α-pinene is in a different position in the molecule, the V247L mutation could improve enzyme−substrate complementarity.

The mutants Y96F, F87A/Y96F, F87L/Y96F, F87W/Y96F, Y96F/V247L, and F87W/Y96F/V247L were examined for the binding and oxidation of (+)-α-pinene. All these mutants were readily expressed and purified to homogeneity and showed similar stability to the wild-type enzyme. A preliminary account of some of this work has been published.[39]

(+)-α-Pinene Binding and Oxidation. The substrate binding and catalytic parameters for (+)-α-pinene oxidation by wild-type P450$_{cam}$ and the active site mutants are collected in Table 2. For comparison the camphor binding constant (K_D) for wild-type P450$_{cam}$ is 0.25 μM. The camphor oxidation rate of the wild-type enzyme is 400 min^{-1} under identical conditions, with >95% coupling, i.e., nearly all the NADH consumed is utilized for the formation of 5-*exo*-hydroxycamphor.[40] Wild-type P450$_{cam}$ and all the mutants showed >70% conversion to high-spin heme upon (+)-α-pinene binding. The structural similarity between

(37) Harford-Cross, C. F.; Carmichael, A. B.; Allan, F. K.; England, P. A.; Rouch, D. A.; Wong, L.-L. *Protein Eng.* **2000**, *13*, 121−128.

(38) Atkins, W. M.; Sligar, S. G. *J. Biol. Chem.* **1988**, *263*, 18 842−18 849.
(39) Bell, S. G.; Sowden, R. J.; Wong, L.-L. *Chem. Commun.* **2001**, 635−636.
(40) Gelb, M. H.; Heimbrook, D. C.; Mälkönen, P.; Sligar, S. G. *Biochemistry* **1982**, *21*, 370−377.

Table 2. Binding and Oxidation of (+)-α-Pinene by Wild-Type (WT) $P450_{Cam}$ and Active-Site Mutants

	WT	Y96F	F87A/Y96F	F87L/Y96F	F87W/Y96F	Y96F/V247L	F87W/Y96F/V247L	F87W/Y96F/L244A/V247L	F87W/Y96F/L244A	Y96F/L244A/V247L
% high spin heme	85	95	70	80	95	95	75	85	65	90
K_D, μM	1.10	0.15	0.12	0.10	0.08	0.14	0.30	0.24	0.26	0.15
NADH turnover rate[a]	82	147	210	163	171	298	129	233	122	223
product formation rate[b]	18.6	56	150	88	96	271	65	156	120	129
coupling efficiency[c]	23%	38%	72%	54%	56%	91%	51%	67%	95%	58%

[a] Given as nanomoles of NADH consumed per nanomole of $P450_{cam}$ per minute. [b] The total amount in nanomole of product formed per nanomole of $P450_{cam}$ per minute. [c] The coupling efficiency is the ratio of the total amount of products formed to the amount of NADH consumed, i.e., the yield based on NADH, and is expressed as a percentage.

Table 3. Distribution of Products (±2%) from (+)-α-Pinene Oxidation Catalyzed by Wild-Type and Active Site Mutants of $P450_{cam}$

$P450_{cam}$ enzyme	(+)-α-pinene epoxides	(+)-*cis*-verbenol	(+)-myrtenol	(+)-verbenone	others
wild-type	4%	31%	4%	10%	51%
Y96F	3%	46%	10%	12%	29%
F87A/Y96F	22%	33%	7%	8%	30%
F87L/Y96F	12%	38%	7%	10%	33%
F87W/Y96F	7%	66%	3%	7%	17%
Y96F/V247L	12%	55%	7%	7%	19%
F87W/Y96F/V247L	3%	70%	4%	8%	15%
F87W/Y96F/L244A/V247L	12%	44%		13%	31%
F87W/Y96F/L244A	2%	86%	2%	5%	5%
Y96F/L244A/V247L	1%	55%		32%	12%

camphor and (+)-α-pinene also meant that wild-type $P450_{cam}$ showed tighter (+)-α-pinene binding, higher oxidation activity, and tighter coupling than for compounds such as styrene,[41−43] ethylbenzene,[44] and linear alkanes,[36] which have very different structures from camphor.

As predicted the Y96F mutation strengthened (+)-α-pinene binding and increased the rate and coupling of oxidation. A hydrophobic substitution at F87, regardless of side-chain volume, further enhanced both the binding and oxidation activity. On the other hand, adding the V247L mutation did not significantly tighten (+)-α-pinene binding but both the rate and coupling were greatly improved. The (+)-α-pinene oxidation rate of 270 min^{-1} for the Y96F/V247L double mutant was ca. 70% of the camphor oxidation activity of wild-type $P450_{cam}$ under identical conditions.

The data showed that there is no direct correlation between the high−spin heme content and the strength of (+)-α-pinene binding or the rate and coupling efficiency. It is also interesting to note that (+)-α-pinene binding by Y96F and a number of multiple mutants was tighter than camphor binding by the wild-type.

(+)-α-Pinene Oxidation Products. Camphor oxidation by wild-type $P450_{cam}$ occurs exclusively at C_5 to give the exo alcohol. If the geminal methyl groups of camphor and (+)-α-pinene were superimposed in the crystal structure, the dominant product should be (+)-*cis*-verbenol (Scheme 1). In addition some (+)-α-pinene epoxide might be expected because the reactive olefinic double bond might also be close to the heme iron.

GC coelution experiments and ^{1}H NMR spectroscopy showed that the major product from (+)-α-pinene oxidation catalyzed by wild-type $P450_{cam}$ and all the mutants was indeed (+)-*cis*-verbenol. However, despite the similar structures of camphor and (+)-α-pinene, the selectivity for (+)-*cis*-verbenol was nowhere near the 100% selectivity for camphor oxidation. Both the cis and trans isomers of (+)-α-pinene epoxide were minor products, identified by coelution with an authentic sample. This is an important observation because it indicated that the (+)-α-pinene substrate was not freely mobile within the active site. If the substrate was freely mobile, the most reactive functional group—the olefinic double bond—would be preferentially attacked and the epoxides would be the major products. (+)-Myrtenol, which arose from oxidation of the C_{10} methyl group, was another minor product identified by GC coelution experiments and its ^{1}H NMR spectrum. (+)-Verbenone, the further oxidation product of (+)-*cis*-verbenol, was also formed. In addition to these characterized compounds there were additional, small peaks in the gas chromatograms. These products were not characterized but some peaks were at retention times consistent with monooxygenated (+)-α-pinene compounds, while the longer retention times of others were consistent with compounds derived from oxidation at multiple carbons.

Scheme 1. Products from (+)-α-Pinene Oxidation Catalyzed by Cytochrome $P450_{cam}$

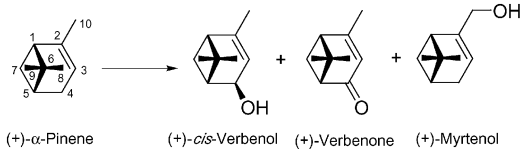

The distribution of (+)-α-pinene oxidation products for the $P450_{cam}$ enzymes is given in Table 3. Wild-type $P450_{cam}$ showed some selectivity for (+)-*cis*-verbenol, but there were many other products, especially compounds at long retention times. The Y96F mutation increased the proportion of (+)-*cis*-verbenol and (+)-myrtenol, mainly at the expense of the multiple oxidation products. The F87A and F87L mutations, which were expected to increase the space available in the active site and potentially increase substrate mobility, increased the amount of epoxides formed. In contrast, the F87W and V247L mutations, which reduced the active site volume, significantly increased the selectivity for (+)-*cis*-verbenol. The effects of these two

(41) Nickerson, D. P.; Harford-Cross, C. F.; Fulcher, S. R.; Wong, L. L. *FEBS Lett.* **1997**, *405*, 153−156.
(42) Fruetel, J. A.; Collins, J. R.; Camper, D. L.; Loew, G. H.; Ortiz de Montellano, P. R. *J. Am. Chem. Soc.* **1992**, *114*, 6987−6993.
(43) Mayhew, M. P.; Reipa, V.; Holden, M. J.; Vilker, V. L. *Biotechnol. Prog.* **2000**, *16*, 610−616.
(44) Filipovic, D.; Paulsen, M. D.; Loida, P. J.; Sligar, S. G.; Ornstein, R. L. *Biochem. Biophys. Res. Commun.* **1992**, *189*, 488−495.

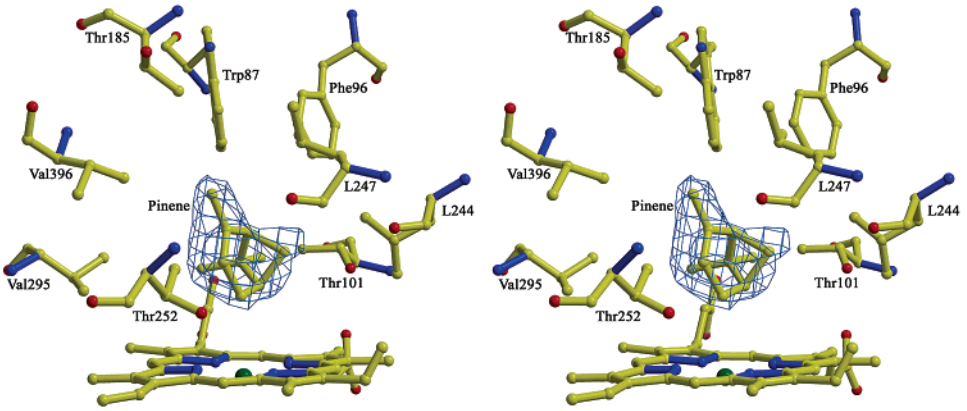

Figure 3. Stereoview of the active site structure of molecule **A** of the F87W/Y96F/V247L mutant of $P450_{cam}$ showing the substrate electron density and the fit to the (+)-α-pinene substrate. The (+)-α-pinene location overlaps that of camphor in the wild-type structure and the (+)-α-pinene orientation can be generated approximately from that of camphor by a number of rotations. See text for details. The figure was generated by MOLSCRIPT and BOBSCRIPT and rendered by RASTER3D.

mutations were not additive—when they were combined the selectivity for (+)-*cis*-verbenol was only increased slightly. Nevertheless the selectivity for (+)-α-pinene oxidation at C_4, i.e., forming verbenol and verbenone, was greatly improved compared to the that for wild-type enzyme, to 78% and 72% respectively for the F87W/Y96F/V247L and F87W/Y96F mutants.

Crystal Structure of the F87W/Y96F/V247L Mutant with (+)-α-Pinene Bound. We determined the 2.3-Å resolution crystal structure of the F87W/Y96F/V247L mutant with (+)-α-pinene bound in its active site. This triple mutant was marginally the most selective of the $P450_{cam}$ enzymes initially studied. The structure should provide insight into the enzyme—substrate contacts and how product selectivity could be further engineered. Crystals of the mutant were obtained by crystallization with PEG8000. The mutant crystallized in the space group $P2_1$, identical to the monoclinic form obtained from PEG4000 and with virtually identical unit cell parameters[27] but different from the orthorhombic crystals from ammonium sulfate.[20]

The structure was solved by molecular replacement based on the phases from the wild-type structure. The two independent molecules (**A** and **B**) in the unit cell were readily located and refined. Most of the C_α backbone and side chains of the two molecules were superimposable on that of the wild-type. The iron was below the plane of the heme (0.36 Å in both molecules **A** and **B**, 0.37 Å in the wild-type) and the iron—cysteine thiolate distances (2.08 Å in **A** and 2.29 Å in **B**) were similar to that in the wild-type (2.20 Å). The key heme—protein contacts found in the wild-type structure were all present.

There were no water molecules in the active site of either mutant molecule in the unit cell. Most of the side-chains in the active site were found in similar or identical orientations to the wild-type, suggesting that the three mutations had little effect on the structure. The (+)-α-pinene substrate was bound in different orientations in the two molecules in the unit cell, but its location in both molecules overlapped significantly with that found for camphor in the wild-type structure.

(+)-α-Pinene Binding in Molecule A. The (+)-α-pinene binding orientation in molecule **A** (Figure 3) was closely related to that found for camphor and camphane in the wild-type structures.[22] Camphor and camphane are located over the meso carbon CHA and the adjacent C1A and C4D of the A and D pyrroles,[20] with the C_8,C_9 methyls above the A pyrrole and in contact with V295. The C_1 atom of (+)-α-pinene was at almost the same location as C_1 of camphor in the wild-type structure. The (+)-α-pinene C_{10} methyl was in van der Waals contact (Table 4) with the side chains of T185, L247, and V396, which were located high up in the substrate pocket. The indole side chain of W87 contacted the (+)-α-pinene C_1, suggesting that this larger side chain compensated for the absence of the camphor carbonyl group. Closer to the heme, the L244 side chain, which played a very important role in camphor binding

Table 4. Contacts (4 Å or Less) between (+)-α-Pinene and the F87W/Y96F/V247L Mutant of $P450_{cam}$ in Molecules **A** and **B**

	molecule **A**		molecule **B**	
(+)-α-pinene	$P450_{cam}$	distance	$P450_{cam}$	distance
C-1	CH2 Trp87	4.00	C1A heme	3.98
	CD2 Leu247	3.90	NA heme	3.71
			C4A heme	3.90
C-2			CA Gly248	3.90
			ND heme	3.70
			NA heme	3.75
C-3	CG2 Thr252	3.20	CA Gly248	3.90
			N Gly248	3.69
C-4	NA heme	3.51	CD1 Leu244	3.55
	ND heme	3.65	CD2 Leu247	3.55
C-5	NA heme	3.70	CH2 Trp87	3.56
	ND heme	3.53		
	CHA heme	3.72		
	C1A heme	3.73		
	C4D heme	3.61		
C-6			C1A heme	3.98
			C2A heme	4.00
C-7	CD1 Leu244	3.65		
C-8	CG1 Val295	3.82	CG2 Thr101	3.98
	C1A heme	3.97	C1A heme	3.34
	C2A heme	3.77	C2A heme	3.48
	C3A heme	3.89	C4D heme	3.98
	CBA heme	3.78	CBA heme	3.00
			CHB heme	3.30
C-9	CG2 Thr101	3.64	CG1 Val295	3.59
			OD2 Asp297	3.61
			CBA heme	3.61
C-10	CG2 Thr185	3.71	C1A heme	3.99
	CD2 Leu247	3.72	C4A heme	3.92
	CG Leu247	3.67	C1B heme	3.96
	CG2 Val396	3.36	NA heme	3.21
			NB heme	3.06
			NC heme	3.00
			ND heme	3.06

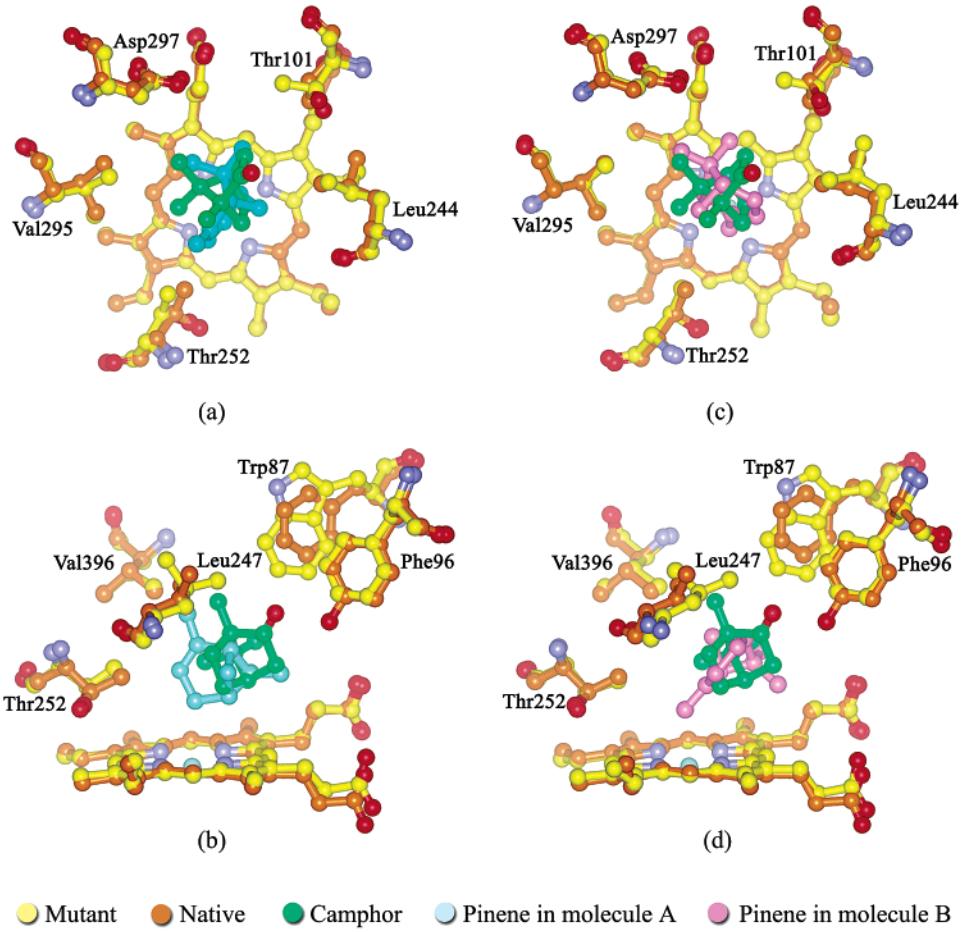

Figure 4. Comparison of the (+)-α-pinene binding location and orientation in molecule **A** (panels a and b) and molecule **B** (panels c and d) of the F87W/Y96F/V247L mutant with that of camphor in the wild-type structure. Panels a and c are views from the top of the active site to emphasize the contacts between (+)-α-pinene and side-chains close to the heme. Panels b and d are views from the side to show the location of the T252 side chain and emphasize contacts with side chains near the top of the active site. The figures were generated by the program WEBLAB VIEWER PRO.

in the wild-type, only contacted the C_7 carbon of (+)-α-pinene in the mutant.

The (+)-α-pinene binding orientation in molecule **A** could be generated from that of camphor in the wild-type structure by aligning the pinene C_1,C_5 vector with the C_1,C_4 vector of camphor and rotating the (+)-α-pinene molecule around this vector by ca. 90°, so that the C_8,C_9 methyl groups moved away from V295 and toward the CHA meso carbon (Figure 4). As a result the C_8 methyl group in (+)-α-pinene contacted the V295 side chain, but the C_9 methyl contacted T101 (Table 4). The rotation was also accompanied by a tilt of the pinene C_1,C_5 vector, with C_5 moving toward the D pyrrole compared to the position of camphor C_4 in the wild-type structure. The combined rotation and tilting placed the C_4 atom of (+)-α-pinene closest to the heme iron. The Fe−C_4 distance was 3.40 Å and the C/Fe/S(C357) angle was 175°, compared with 3.40 Å and 164° for camphor C_5 in the wild-type structure.[20] The exo face at C_4 was closer to the iron than the endo side. The predicted product would therefore be (+)-*cis*-verbenol. We note that, if no tilting of (+)-α-pinene relative to camphor occurred, the rotation on its own would have brought the exo side at C_4 past the iron. The endo side would then be closer to the oxygen of the ferryl intermediate, and (+)-*trans*-verbenol would have been the major product.

(+)-α-Pinene Binding in Molecule B. The electron density map and fit for the (+)-α-pinene substrate in molecule **B** is shown in Figure 5. This unexpected orientation was related to that in molecule **A** by a ca. 180° rotation about the vector bisecting the C_8,C_6,C_9 plane (Figure 4). The C_1 and C_{10} atoms moved from the top of the active site to positions close to the heme. The C_8 and C_9 methyls effectively switched positions compared to molecule **A**, such that C_8 in molecule **B** contacted T101, while C_9 contacted V295 (Table 4). In addition, the (+)-α-pinene molecule moved toward pyrrole **A** such that C_9 was close to one of the carboxylate oxygens of D297, and both C_8 and C_9 were in contact with CBA of the propionate group on pyrrole **A**.

The carbon atom closest to the iron was the C_{10} methyl (2.70 Å, C/Fe/S angle 170°), and (+)-myrtenol should be the major product.

Enzyme−Substrate Contacts and Implications in Coupling and Product Selectivity. The initial assumption in designing $P450_{cam}$ active-site mutations was that the structural resemblance to camphor should allow (+)-α-pinene to bind in a similar orientation to that found for camphor in the wild-type. This was largely the case in molecule **A** but not in molecule **B**. Indeed the (+)-α-pinene/enzyme contacts in both molecules were significantly different from those in the wild-type structure. Due to the rotation of (+)-α-pinene in molecule **A** relative to the camphor binding orientation in the wild-type, only one, rather than both, of the C_8,C_9 methyl groups contacted V295. The side-chains at the 87, 96, and 244 positions, which were

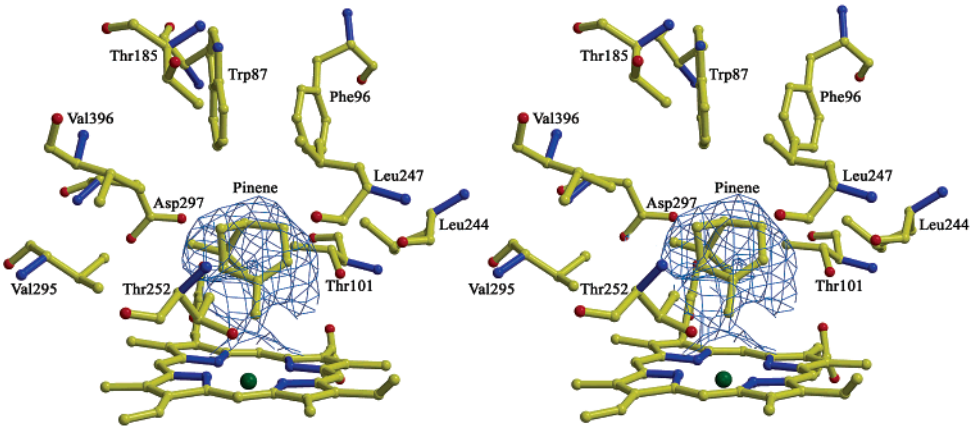

Figure 5. Stereoview of the active-site structure of molecule **B** of the F87W/Y96F/V247L mutant of $P450_{cam}$ showing the substrate electron density and the fit to the (+)-α-pinene substrate. The (+)-α-pinene location overlaps that found in molecule **A** and of camphor in the wild-type structure. The (+)-α-pinene orientation can be generated approximately from that in molecule **A** by rotation. See text for details. The figure was generated by MOLSCRIPT and BOBSCRIPT and rendered by RASTER3D.

prominent in camphor binding by the wild-type,[20] were much less involved in (+)-α-pinene binding by the mutant. In contrast the T101 side-chain was not involved in camphor binding in the wild-type, but in the mutant it contacted one of the (+)-α-pinene geminal methyl groups. There were also more (+)-α-pinene/heme contacts in both molecules than between camphor and the heme, in particular in molecule **B** (Table 4).

The absence of water molecules in the active site of the mutant with (+)-α-pinene bound was consistent with the large shift of the heme spin state to high spin and the relatively high coupling efficiency of 51%. However, since there was no evidence for the binding of water to the heme iron in either molecule, the crystal structure did not offer an explanation to why the heme was not fully high spin. A possible explanation is that the structure was determined at −100 °C, while the heme spin state was measured at 30 °C. At this higher temperature it is very likely that the (+)-α-pinene molecule undergoes dynamic motions and, in some binding orientations, water may bind to the iron to give a population of low-spin heme.

Dynamic substrate binding and the entry of water to bind to the heme iron may partially explain why the coupling for (+)-α-pinene oxidation by the F87W/Y97F/ V247L mutant was lower than might be expected from the crystal structure. Thus access of water to the heme iron during the catalytic cycle could lead to protonation of the ferric peroxide intermediate at the heme-bound oxygen and subsequent loss of hydrogen peroxide.[45] In addition, Sligar and Poulos have both suggested that substrate mobility, regardless of whether water was bound to the heme iron in some population of the enzyme, may also lead to uncoupling.[22,45] This mechanism was expected to become more important if some of the interconverting binding orientations, or movement between them, involved close approach of the substrate to the heme-bound oxygen species. Of the two observed (+)-α-pinene binding orientations, that in molecule **A** resembled that of camphor in the wild-type and little uncoupling was expected. On the other hand the close approach of the C_{10} methyl group to the heme iron in molecule **B** could interfere with the iron−oxygen interaction, leading to uncoupling. Furthermore the crystal structure suggested that the most direct and likely pathway for the interconversion between the two orientations would be a ca. 180° rotation about the vector bisecting the C_8,C_6,C_9 plane (Figure 4). During this process the C_{10} methyl would traverse the space between the heme iron and the T252 side chain, which had been proposed to be the oxygen binding pocket,[21] and uncoupling was expected.

Identification of substrate binding orientations allowed predictions of the (+)-α-pinene oxidation products. We would predict that (+)-*cis*-verbenol should be the major product from molecule **A**, and for molecule **B** (+)-myrtenol should be the major product. Experimentally we found that the proportion of (+)-*cis*-verbenol (70%) far exceeded that of (+)-myrtenol (4%). Since interconversion between the two binding orientations was expected at the assay temperature, this result might simply reflect the higher reactivity of the sp^2 C−H bonds at C_4 compared to the sp^3 bonds at C_{10}. Alternatively, the expected uncoupling for the binding orientation in molecule **B** might also reduce the amount of (+)-myrtenol formed. In addition, we cannot rule out the possibility that the binding orientation in molecule **A** was slightly more stable and therefore more prevalent in solution at the assay temperature.

Another factor is the known movement of camphor during the catalytic cycle. Camphor moves toward the heme *meso* carbon CHA in the wild-type structure to make room for oxygen to bind to the ferrous heme.[27] After O−O bond activation and formation of the ferryl intermediate, camphor moves back toward the iron.[27] During this process the exo face at C_5 is always closer to the iron, and 5-*exo*-hydroxycamphor is the only product. In an analogous manner we would expect the binding orientation in molecule **A** to be maintained and give (+)-*cis*-verbenol as the product. The situation for molecule **B** is more complicated because the C_{10} methyl was very close to the iron and had to move over a longer distance upon oxygen binding. The interesting question is whether this movement resulted in other orientations being adopted; e.g., a certain population of pinene molecules in molecule **B** might adopt the orientation found in molecule **A**, thus leading to more (+)-*cis*-verbenol. It is also easy to envisage orientations which would bring the olefinic double bond close to the iron, resulting in epoxide formation. We believe that a combination of the inherent reactivity of the pinene C−H bonds and substrate movement during the catalytic cycle probably accounted for the observed product distribution.

(45) Loida, P. J.; Sligar, S. G. *Biochemistry* **1993**, *32*, 11 530−11 538.

Further Engineering of P450$_{cam}$. Based on the crystal structure of the F87W/Y96F/V247L mutant and the selectivity of the other mutants, we sought combinations of mutations which might further increase the selectivity for (+)-*cis*-verbenol formation. The selectivity data clearly showed that the Y96F, F87W, and V247L mutations all promoted the formation of (+)-*cis*-verbenol, with the F87W mutation apparently having the greater effect. However, the effects of the F87W and V247L mutations were not additive. The crystal structure suggested a plausible explanation: the leucine side-chain at the 247 position contacted the C_{10} methyl and pulled the (+)-α-pinene molecule away from the side-chain at the 87 position. In other words there was competition rather than cooperation between the effects of the F87W and V247L mutations.

We sought to increase the selectivity for (+)-*cis*-verbenol formation by disfavoring the binding orientation in molecule **B**. The enzyme/substrate contacts from the crystal structure suggested that this might be possible if the (+)-α-pinene molecule was to move toward pyrrole D, thus weakening or breaking the contacts with the D297 side-chain and the propionate CBA carbon. The L244 side chain was targeted because it was located over pyrrole D and it also contacted the (+)-α-pinene molecule. We therefore introduced the L244A mutation and prepared the F87W/Y96F/L244A/V247L, F87W/Y96F/L244A, and Y96F/L244A/V247L mutants, which also allowed us to explore the possible competition between the effects of the F87W and V247L mutations. The (+)-α-pinene oxidation activity and selectivity of these new mutants are given in Tables 2 and 3.

Addition of the L244A mutation increased the activity of the F87W/Y96F and F87W/Y96F/V247L mutants but not the Y96F/V247L mutant. When the V247L mutation was present, the L244A mutation had little effect on the strength of pinene binding. On the other hand the F87W/Y96F/L244A mutant showed much weaker pinene binding than the F87W/Y96F parent mutant. Interestingly, the tight coupling of the F87W/Y96F/L244A mutant did not require the complete shift of the heme spin state to high spin. This result mirrored that of camphor oxidation by the Y96F mutant, where complete coupling was observed for a 55% high-spin heme content in the camphor-bound form.[38] The L244A mutation also had significant effects on the selectivity, notably reducing the amount of (+)-myrtenol formed. Moreover, the F87W/Y96F/L244A mutant gave 86% (+)-*cis*-verbenol, the highest selectivity of all the P450$_{cam}$ mutants studied. With 5% of (+)-verbenone also formed, the overall regioselectivity for C_4 attack was 91%. This high selectivity and tight coupling (>95%) were close to those for camphor oxidation by the wild-type, although the product formation rate was lower. The Y96F/L244A/V247L mutant gave 55% (+)-*cis*-verbenol and 32% (+)-verbenone, and there was one major side product (ca. 10%) at a long retention time. The data for the new mutants suggested that the binding orientation in molecule **B** was disfavored by the L244A mutation but not when both the F87W and V247L mutations were present, again reflecting the competition between the effects of these two mutations.

We found that (+)-*cis*-verbenol was further oxidized to (+)-verbenone to various extents by all the P450$_{cam}$ enzymes studied, especially the Y96F/L244A/V247L mutant, even though (+)-α-pinene was present in excess. This was not the case for camphor oxidation by the wild-type and the Y96F mutant[38] or any of the mutants studied here; 5-oxocamphor was not formed until >95% of the camphor had been consumed. Further oxidation would occur if binding of the initial alcohol product could compete with binding of the starting substrate. Camphor binding by wild-type P450$_{cam}$ is more than an order of magnitude tighter than the binding of 5-*exo*-hydroxycamphor.[29] It has been reported that in vivo camphor oxidation in *E. coli* by a triple fusion protein, in which P450$_{cam}$ was fused with its two physiological electron-transfer partner proteins, gave 5-oxocamphor before camphor was exhausted.[46] The change from in vitro to in vivo conditions could have resulted in the increased double oxidation of camphor. However, another in vivo P450$_{cam}$ system, in which the three proteins were separately expressed and thus freely diffusing inside the *E. coli* cytoplasm, did not give the ketone before camphor exhaustion.[47] These data indicated that there was a smaller difference between the strength of camphor and 5-*exo*-hydroxycamphor binding by the P450$_{cam}$ domain in the triple fusion protein, perhaps arising from structural changes induced by fusing P450$_{cam}$ with the electron-transfer proteins in a single polypeptide. It is not clear why the combination of mutations in the Y96F/L244A/V247L mutant also narrowed this difference in binding so that this mutant was more effective in double oxidation of (+)-α-pinene to (+)-verbenone than the Y96F/V247L and F87W/Y96F/L244A mutants. Unraveling the intricate enzyme/substrate interactions and associated dynamics that give rise to this complex activity pattern will require further investigations, including X-ray crystallography. However, the results suggest that it should be possible to engineer a P450$_{cam}$ mutant that will stop the oxidation at (+)-*cis*-verbenol, while another mutant could oxidize (+)-α-pinene to (+)-verbenone even in the presence of excess pinene.

Conclusions

The heme monooxygenase cytochrome P450$_{cam}$ has been re-engineered for the oxidation of (+)-α-pinene which is structurally related to camphor, the natural substrate of the enzyme. Consideration of the structures of these two molecules lead to mutants with enhanced activity and product selectivity for (+)-α-pinene oxidation. The crystal structure of the Y96F/F87W/V247L mutant provided new insight into P450$_{cam}$ substrate binding and catalysis. Analysis of the enzyme−substrate interactions and dynamics lead to the introduction of the L244A mutation, which increased the selectivity for (+)-*cis*-verbenol to 86% for the F87W/ Y96F/L244A mutant, but unexpectedly there was significant further oxidation by the Y96F/L244A/V247L mutant, which gave 32% (+)-verbenone. The P450$_{cam}$ system has also been expressed in *E. coli* to provide whole-cell, in vivo substrate oxidation systems.[46,47] With some improvements in selectivity, engineered P450$_{cam}$ mutants may have applications in the biotransformation of (+)-α-pinene. Finally the results of the present work also suggest that the current understanding of P450 catalytic activity allows the design of mutations to increase the rate of oxidation of many unnatural substrates on the basis of the hydrophobicity, size, shape, and rigidity of the target compound. However, the much more

(46) Sibbesen, O.; De Voss, J. J.; Ortiz de Montellano, P. R. *J. Biol. Chem.* **1996**, *271*, 22 462−22 469.
(47) Bell, S. G.; Harford-Cross, C. F.; Wong, L. L. *Protein Eng.* **2001**, *14*, 797−802.

demanding challenge is in engineering the regioselectivity and stereoselectivity of substrate oxidation because the $P450_{cam}$/substrate molecular recognition interactions are both highly dynamic and subtly modulated by amino acid substitutions.

Acknowledgment. This research was supported by the following grants from the National Science Foundation of China (to Z.R.): Project "973" No. G1999075602 and Project "863" No. 2001AA233011. We thank the support of the Biotechnology and Biological Sciences Research Council, U.K. (Grant Reference B10666), and the Engineering and Physical Sciences Research Council, U.K. (Studentship to R.J.S.). We also thank the Referees for helpful suggestions.

JA028460A